Journal of Robotics and Control (JRC)
Volume 4, Issue 4, 2023
ISSN: 2715-5072, DOI: 10.18196/jrc.v4i4.18208

ROS-based Controller for a Two-Wheeled Self-Balancing Robot

Juan Díaz-Téllez [1], Ruben Senen García-Ramírez[2], Jairo Pérez-Pérez [3],
Jaime Estevez-Carreón [4*], Miguel Angel Carreón-Rosales[5]
Electronics Dept., National Technology Institute of Mexico/"Instituto Tecnológico de Puebla", Pue MX
Email: [1] juan.diaz@puebla.tecnm.mx, [2] rubensenen.garcia@puebla.tecnm.mx, [3] jairo.perez@puebla.tecnm.mx,
[4] jaime.estevez@puebla.tecnm.mx, [5] miguelangel.rosales@puebla.tecnm.mx
*Corresponding auhtor

***Abstract*—In this article, a controller based on a Robot Operating System (ROS) for a two-wheeled self-balancing robot is designed. The proposed ROS architecture is open, allowing the integration of different sensors, actuators, and processing units. The low-cost robot was designed for educational purposes. It used an ESP32 microcontroller as the central unit, an MPU6050 Inertial Measurement Unit sensor, DC motors with encoders, and an L298N integrated circuit as a power stage. The mathematical model is analyzed through Newton-Euler and linearized around an equilibrium point. The control objective is to self-balance the robot to the vertical axis in the presence of disturbances. The proposed control is based on a bounded saturation, which is lightweight and easy to implement in embedded systems with low computational resources. Experimental results are performed in real-time under regulation, conditions far from the equilibrium point, and rejection of external disturbances. The results show a good performance, thus validating the mechanical design, the embedded system, and the control scheme. The proposed ROS architecture allows the incorporation of different modules, such as mapping, autonomous navigation, and manipulation, which contribute to studying robotics, control, and embedded systems.**

***Keywords*—ROS; Mobile robot; Two-wheeled self-balancing; ESP32; Segway.**

I. Introduction

In recent years, autonomous mobile robots have been a matter of research in the academy and industry. Due to their maneuverability, precision, autonomy, loading capacity, and flexibility, the mobile robots have been used for different tasks, for example, in agriculture [18], [19], [20], drawing applications [25], [26], [27], personal mobility [36], [37], [38], cooperative tasks [21], [22], [23], [24], package delivery [28], [29], surveillance [30], [31], [32], [33] and search and rescue [34], [35].

Mobile robots have different configurations depending on the type of wheels used (drive, passive and omnidirectional) and design. For example, mobile robots with differential drive [1], [2], [3], [4], [5], [6] Ackermann steering drive [7], [8], [9], [10] and omnidirectional drive [11], [12], [13], [15], [16] [14]. Nevertheless, the development of new configurations has grown rapidly in the last decade.

In particular, mobile inverted pendulum robots (MIPR) have been widely accepted in different applications. Its two independent drive motors allow it to balance and drive in a straight line, turn on its axis, curve, and cross small slopes. From a control perspective, MIPRs are unstable, nonlinear, and underactuated systems [17].

In the scientific literature, we can find different control algorithms for mobile robots. Most dedicated to the design of linear and time-invariant controls (LTI). For example, in [39], [40], [41], [42], [43], [44] a proportional-integral-derivative PID control is proposed. An optimal quadratic linear regulator LQR at [45], [47], [48], [49], [50]. A cascade proportional-derivative control with a proportional-integral control is proposed in [41].

In [46], two controls for a MIPR are designed to compare their performance, a PID controller and an optimal LQR controller. The results show a settling time of 0.3 seconds in the PID, a steady state error close to zero with an overdamping of 20 %. In addition, it only allows a deviation error of 5 degrees from the vertical axis of the pendulum. On the other hand, the optimal LQR control shows better results, reducing the overshoot observed in the PID and improving the response in a steady and transient state.

Because LTI controls are susceptible to external disturbances, unmodeled dynamics, and uncertainties, different nonlinear control strategies have been designed. For example, Backstepping [51], [52], [53], [54]. Sliding mode control (SMC) [55], [56], [57], [58], adaptive control [63], [60], [62], [61], [63], fuzzy logic control in [69], [67], [68], [66], and antidisturbance control [64], [65]. However, with the increasing complexity of the tasks assigned to this type of robot, it is necessary to implement effective communication between their processes.

The Robot Operating System (ROS) is a set of software libraries and tools that help you build robot applications. ROS acts as a meta-operating system for robots, providing hardware

abstraction, low-level device control, inter-processes message-passing, and package management [81]. ROS allows you to manage the different layers and parallelize the processes and their communication with sensors, actuators, and processing units. Few papers cover ROS middleware for robot scalability. Some ROS-based works can be found at [72], [73], [74], [76], [77], [78]. For example, in [70] proposes implementing the ROS service to generate polynomial trajectories. Results are made in the open field for an agricultural robot. To the same extent, an adaptive Monte Carlo Localization (AMCL) algorithm is designed to navigate a mobile robot indoors in [80].

At [71], a ROS-based control for a UGV with a handling arm is used autonomously for early pest detection and selective treatment tasks. In [79], a mobile robot is used to build a map of the robot's physical environment. A SLAM algorithm and a Unity3D environment are used with the ROS middleware. In [75], a route planner is designed together with a control of pose regulation based on ROS for an Ackerman mobile robot. Physical tests demonstrate ROS-based navigation and control capabilities for agriculture applications.

The research topic and the contribution of this work focus on developing an open architecture based on ROS that allows the integration of different modules such as control, manipulation, navigation, and perception for mobile robots. This architecture contains sensors, a low-level controller, and a communication layer. This architecture reduces the development time to perform robotic applications due to the efficient reuse of standard modules and robot platforms. To validate the ROS-based architecture, a bounded saturation LTI controller is proposed. The proposed controller is compared with the classical PID and LQR approaches. The main contributions are numbered below,

- A ROS-Based embedded control is designed.
- Design of a low-cost prototype for educational purposes.
- Development of the embedded system, instrumentation, and control.
- The algorithm is relatively easy to implement in an embedded system.
- Real-time tests are performed to validate the control law.

It is worth mentioning that several scale prototypes developed at the Tecnológico Nacional de México/Instituto Tecnológico de Puebla TECNM/ITP, which serve as the subjects of the specialty module. It helps us introduce concepts of stability, modeling, nonlinearities, control, power electronics, programming, embedded systems, and computer-aided design CAD. The rest of the document is structured as follows. Section II presents the mathematical model of the two-wheeled self-balancing mobile robot. Section III is its mechanical and electronic design. In section IV, the controller is addressed. Section V numerical simulations and experimental results are illustrated. Finally, the conclusions and future work in section VI are given.

II. Two-Wheeled Self-Balancing Mathematical Model

This section presents the nonlinear mathematical modeling of the two-wheeled self-balancing mobile robot. The nonlinear dynamic model of the WIPR is obtained employing Newton's formulation.

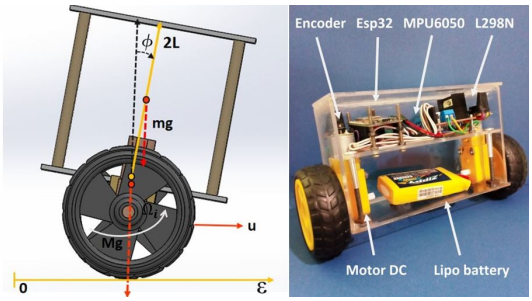

Fig. 1. Two-wheeled self-balancing a) Free-body diagram. b) Implemented prototype.

In this work, the stabilization of the robot to its vertical position against external disturbances is addressed. Consider the free-body diagram in Fig. 1 (a). The following equations give the equations that describe the dynamics of the inverted pendulum angle and the displacement of the mobile robot.

$$\ddot{\xi} = \frac{\left(m^2l^2g\sin 2\phi\right)/2-\left(J+ml^2\right)(ml\sin\phi)\dot{\phi}^2-\left(J+ml^2\right)u}{aml\cos^2\phi-4l/3} \quad (1)$$

$$\ddot{\phi} = \frac{-(M+m)(mlg\sin\phi)+\left(m^2l^2\dot{\phi}^2\sin 2\phi\right)/2+(ml\cos\phi)u}{aml\cos^2\phi-4l/3} \quad (2)$$

where ξ, and ϕ define the state variables of our system. ξ represents the displacement of the robot ,and ϕ represents the angle of the pendulum. u represents the force exerted by the DC motors and, therefore, on our control input. The inertia of the robot is represented by J, l represents the length of the bar at the centre of mass, M the mass of the robot's base, m is the mass of the bar together with the person on board; finally g represents gravity.

III. Two-Wheeled Self Balancing Mobile Robot Design

A two-wheeled self-balancing robot was designed and developed at the Embedded System Laboratory at the Instituto Tecnológico de Puebla to perform the necessary stability tests. Fig. 1 (b) shows the designed prototype. The system has been divided into mechanical structure, propulsion, embedded system, and communication system.

- Mechanical structure. The mechanical structure of the mobile mini robot consists of a 3 mm caliber acrylic with the following dimensions: 15.5 cm × 6 cm × 10 cm.
- Propulsion system. The propulsion system comprises two 5V permanent magnet direct current motors, and is fitted with a slotted infrared encoder sensor and encoder disk.

The supply voltage is 7 V, with a 1000 mah 2s Zippy Lipo Battery and an L298N H-bridge as the power stage. The L298N has digital inputs with levels from 0 to 5 volts for speed control through the PWM signal and the direction of rotation of the motor. The duration of the Lipo Battery is approximately 1 hour of autonomy of the robot without load.

- Emdedded system. The embedded system is composed of sensing, control and actuation. A 32-bit dual-core ESP32 microcontroller DEVKIT V1 model, with a 240 MHz clock frequency and 16 independent channels to generate pulse width modulation PWM signals with 16 bits resolutions. This chip contains wireless communication modules such as WiFi and Bluetooth. An MPU6050 Inertial Measurement Unit with 6 degrees of freedom (DoF) that combines a 3-axis accelerometer and a 3-axis gyroscope is used as the primary sensor. The MPU6050 is connected to a I^2C communication interface. A complementary filter is used to estimate the pitch angle ϕ. In addition, the reading of the encoder coupled to the motor allows the wheel angle θ to be obtained.
- Communication system. The communication is carried out through distributed computing through ROS, allowing different tasks to run in parallel on other processors, computers, or servers. Fig. 2 shows the proposed communication; the mobile robot reads the sensors, calculates the control algorithm, and publishes its pose through a publisher node. The computer subscribes to the node, graphs it in real-time, saves and displays the information, and finally publishes the desired navigation commands. Communication is done through the WiFi port of the ESP32 to the PC ground station. The measurement of state, filtering, and control algorithm calculation is performed at 100 Hz.

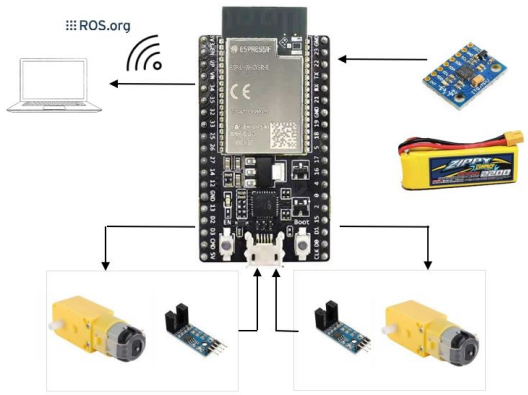

Fig. 2. ROS Communication System.

IV. Control Design.

The system consists of three blocks, an approximate linearization control, an assignment control, and a PID for the dynamics of the DC motor. Fig. 3 shows the control algorithm proposed. The control law is calculated, and the control signal obtained u is converted by the assignment control block into desired movements of the robot, and the speed in both motors Ω_i passes to a PID controller that stabilizes speed of the DC motors. The PID controller is parametrized by PWM signal σ_i. The subscript $= (r, l)$ is for the left and right wheels, respectively.

A. Control Law

The main objective of the control law is the auto-balance, regulate the position of the bar $\phi(t)$ to the desired reference ϕ_d while the angular velocity $\dot{\phi}(t)$ approaches zero when time tends to infinity. Mathematically is expressed as:

$$\phi(t) \to \phi_d, \dot{\phi}(t) \to 0, \text{as} \quad t \to \infty. \tag{3}$$

Let us consider a simplified model of the system described above by decoupling the orientation dynamics. In this case, we present the following second-order system.

$$\dot{x}_1 = x_2 \tag{4}$$

$$\dot{x}_2 = \frac{g \sin x_1 - aml x_2^2 \sin 2x_1 - a \cos x_1 u}{4l/3 - aml \cos^2 x_1} \tag{5}$$

where $x_1 = \phi(t)$ is the pitch angle, measured in radians concerning the vertical, $x_2 = \dot{\phi}(t)$ is the associated angular velocity, and $a = \frac{1}{M+m}$ is a constant.

Considering that the robot remains operating close to the equilibrium point, that is, on the vertical axis, i.e., $x_\delta = \begin{bmatrix} x_{\delta,1} & x_{\delta,2} \end{bmatrix} = \begin{bmatrix} 0 & 0 \end{bmatrix}, u_\delta = 0$ the Jacobian linearization around the equilibrium point results in the LTI form:

$$\dot{x}_\delta = \mathbf{A} x_\delta + B u_\delta + \zeta(t) \tag{6}$$

with

$$A = \begin{bmatrix} 0 & 1 \\ \frac{g}{4l/3 - aml} & 0 \end{bmatrix} \tag{7}$$

$$B = \begin{bmatrix} 0 \\ \frac{-a}{4l/3 - aml} \end{bmatrix} \tag{8}$$

where X_d is the desired angle, $\zeta(t)$ represents endogenous and exogenous disturbance. The new state variables being defined as $x_{1\delta} = x_1 - X_d$, $x_{2\delta} = x_2$, $u_\delta = u_1 - U$ and $U = \frac{g}{a} X_d$.

We verify that the system is controllable,

$$C = \begin{bmatrix} B; AB \end{bmatrix} = \begin{bmatrix} 0 & -\frac{a}{4l/3 - aml} \\ -\frac{a}{4l/3 - aml} & 0 \end{bmatrix} \tag{9}$$

since the determinant is different from zero, then the system is controllable. Linear feedback allows the poles of the closed-loop system to be located at preselected points in the complex plane.

We propose the following desired polynomial,

$$p_d(s) = s^2 + 2\zeta w_n s + w_n^2 \tag{10}$$

the constants ζ, w_n are the damping factor and the undamped natural frequency, respectively.

The feedback control of the state vector is as follows,

$$u = -k_1 x_{1\delta} - k_2 x_{2\delta} + \frac{g}{a} X_d \tag{11}$$

of the desired polynomial, the feedback gains are left as

$$k_1 = -\frac{2\zeta w_n(4l/3 - aml)}{a}, k_2 = -\frac{w_n^2(4l/3 - aml) + g}{a} \tag{12}$$

Since, in practice, it is necessary not to saturate the actuators, we propose adding a bounded function to the control.

Definition 1: Given a positive constant M, a defined by $\sigma_M : \mathbb{R} \to \mathbb{R}$ is defined as:

$$\begin{array}{l}(1)\sigma_M = s \text{ if } |s| < M; \\ (2)\sigma_M = M \cdot \text{sign}(s)\ ;\end{array} \tag{13}$$

Therefore, the implemented controller is:

$$u_a = \sigma_M(-k_1 x_{1\delta} - k_2 x_{2\delta} + \frac{g}{a} X_d) \tag{14}$$

B. Proportional-Integral-Derivative PID Motor Speed Control

A fast and smooth response is necessary for high performance of WIPRs rotational and translational control. The control goal is to design a PID in such a way that the PWM signal makes $lim_{t\to\infty} \mid \Omega_d(t) - \Omega(t) \mid = 0$. The mathematical model of the DC motor can be described as in [42], where its transfer function describes the angular velocity Ω_i with the input voltage to the motor *v*,

$$\frac{\Omega(s)}{v(s)} = \frac{K_m}{LIs^2 + (RI + LB)s + RB + K_m K_a} \tag{15}$$

where *I* represents the rotor's moment of inertia, *R* the electrical resistance, *L* the electrical inductance, *B* represents the motor's viscous friction constant, K_a represents the electromotive force constant, K_m represents the motor torque constant. The manufacturer's parameters for the DC motor used are listed in Table I.

A classic PID control is designed to control the angular speed of the motor Ω_d using as input the voltage v_i parameterized with a PWM signal σ_i.

$$v(t) = k_p e_\Omega(t) + k_i \int e_\Omega(t)dt + k_d \frac{de_\Omega(t)}{dt} \tag{16}$$

where $e_\Omega(t) = \Omega_d - \Omega(t)$, the controller was designed using the Ziegler-Nichols self-sustaining oscillation method. The values obtained are $K_p = 5.8$, $k_i = 19$, $k_d = 0.03$

TABLE I
PARAMETERS

Symbol	Description	Value	Units
I	Moment of inertia	0.000031	kg $\cdot m^2$
R	Armature Resistance	0.425	Ω
L	Electrical inductance	0.00018	H
B	Viscous Friction Constant	0.00028	N $\cdot$ m $\cdot$ s
K_a	Electromotive Force Constant	0.0292	N $\cdot$ m/A
K_m	Motor Torque Constant	0.0281	N $\cdot$ m/A
M	Mobile robot base mass	0.48	Kg
m	Pendulum mass	0.16	Kg
l	Pendulum length	0.25	m
J	Moment of inertia of the mobile robot	0.0043	kg m^2
g	Gravity	9.81	m/s^2

C. Allocation Control

According to some optimization algorithms, the allocation control calculates the angular speeds of the DC motors Ω_i to the desired control inputs or commands. The limitations or constraint conditions of the actuator can be guaranteed,

$$\Omega_{r,d} = u_a(t) + \epsilon_r \tag{17}$$

$$\Omega_{l,d} = u_a(t) + \epsilon_l \tag{18}$$

where the variables $\epsilon_r and \epsilon_l$ are zero if the robot goes in a straight line, and if the robot turns to the right or left, the values are different from zero.

V. Simulation and Experimental Results

Simulation and real-time tests are performed to validate the control architecture based on ROS design. The Kalman controller and filter have been programmed with C++ on the ESP32 microcontroller. The ROS communication between the different nodes has been implemented in C++ as well. Three scenarios have been addressed to validate, compare and measure the performance of the proposed controller. The first scenario demonstrates the ability of the control algorithm to stabilize the robot at the equilibrium point regardless of the initial conditions. In the second scenario, the orientation of the robot is regulated, that is, the position of the bar to the vertical axis. In the third scenario, we compare our controller with PID and LQR algorithms. We also measure the ability to reject endogenous and exogenous disturbances and follow different trajectories. The integral index of squared error ISE is used as a performance index. A saturation function has been used not to exceed the torques supplied to the DC motors. The saturation at the output u_a is in the range of -6 Newton to 6 Newton.

A. Simulations

In this subsection, we perform the numerical simulations of the proposed control algorithm in the MATLAB/Simulink environment.

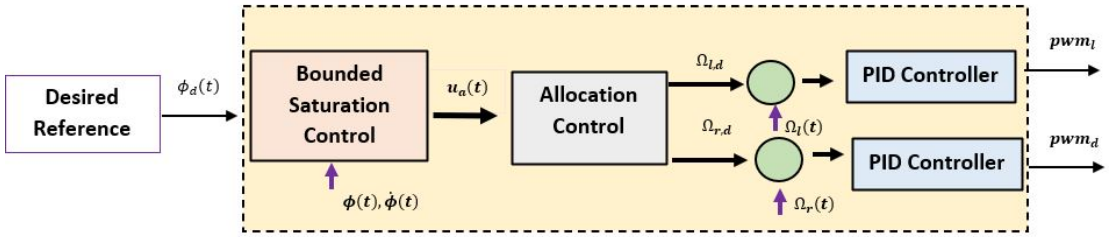

Fig. 3. Block diagram of the two-wheeled self-balancing robot control system.

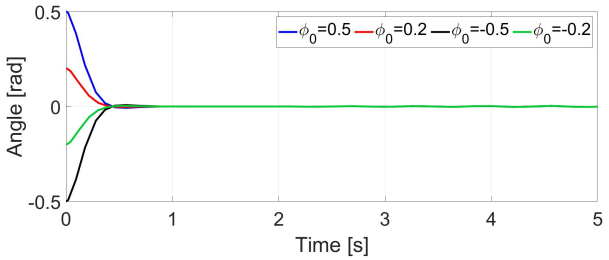

Fig. 4. First scenario: stabilization at the origin.

1) First scenario: The Fig. 4 shows stabilize the pendulum to the vertical axis even when conditions are far from the equilibrium point. The initial values used were $(0.5, 0.2, -0.2, -0.5)$ radians. The response is smooth, fast, and without overshoot. The settling time is approximately 0.5 seconds.

2) Second scenario: Adjustments to different desired angles ϕ_d are performed as a second test. The desired reference are $\phi_d = (0.4, 0.6, -0.4, -0.6)$ radians. We have added an external disturbance to the robot dynamics $\zeta(t) = 3 \sin 0.1t \cos 10t$ rad/sec possibly caused by the wind, friction with the surface, engine wear, or tire slip. Fig. 5 shows that the control can regulate to the desired reference despite external disturbance.

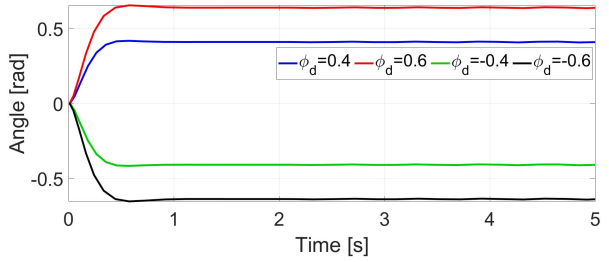

Fig. 5. Second scenario: adjustment to the desired position.

3) Third scenario: A comparative investigation in numerical form is carried out of the proposed algorithm. A classic PID control and an LQR are used to compare the proposed controller. The three algorithms control are simulated in Matlab/Simulink software. The integral square error (ISE), integral time square error (ITSE), integral absolute error (IAE), and integral time absolute error (ITAE) performance indexes are used to analyze the performance of each controller. The performance indexes are expressed by

$$ISE = \int_0^T e_\phi^2(t) \cdot dt \tag{19}$$

$$ITSE = \int_0^T te_\phi^2(t) \cdot dt \tag{20}$$

$$IAE = \int_0^T |e_\phi(t)| \cdot dt \tag{21}$$

$$ITAE = \int_0^T |te_\phi(t)| \cdot dt \tag{22}$$

PID type compensator design methods are very important in stabilizing real systems that operate near equilibrium points. From (7), (8), we calculate the open-loop transfer function.

$$G(s) = \frac{a}{(4l/3 - aml)s^2 - g} \tag{23}$$

The classical form of the PID compensator that stabilizes the output at the equilibrium point is given by the expression:

$$u_{pid}(t) = k_1 e_\phi(t) + k_2 \int e_\phi(t)dt + k_3 \frac{de_\phi(t)}{dt} \tag{24}$$

where $e_\phi(t) = \phi_d - \phi(t)$. The values obtained are $K_1 = 93$, $k_2 = 90$, $k_3 = 10$ via Ziegler-Nichols self-sustaining oscillation.

LQR is an optimal control, which requires complete knowledge of the state. The goal of the controller is to minimize the next performance index.

$$J(x,t) = \frac{1}{2} \int_0^\infty (x^T Q x + u^T R u)dt \tag{25}$$

Equation (25) represents a trade-off between the state's distance from the reference and the cost of the control input. By choosing the matrices Q and R, we can regulate the orientation of the TWSBR.

$$u_{lqr} = Kx_\delta = R^{-1}B^T P x_\delta \tag{26}$$

where $k1 = -55.784$, and $k2 = -2.0445$, besides P is the Riccati matrix equation solution:

$$A^T P + PA - PBR^{-1}B^T P = 0 \tag{27}$$

- Trajectory tracking of a square signal. The desired trajectory is defined by

$$\phi_d(t) = \begin{cases} 0.33 & : 0 \leq t \leq 3 \\ 0 & : 3 \leq t \leq 5 \end{cases} \tag{28}$$

The trajectory can be generated by a rider, ensuring the correct functioning of the robot. Fig. 6 shows the three control algorithms. All three controls are capable of following small time-varying references. The PID control performs poorly since its response is oscillatory and shows errors in a steady state. The LQR control presents a similar response to the proposed controller. However, calculating the gains is more tedious and expensive in processing time. Table II shows the performance indices for the three controls. It can be concluded that the proposed control has better performance, a quicker recovery rate, and less error fluctuation.

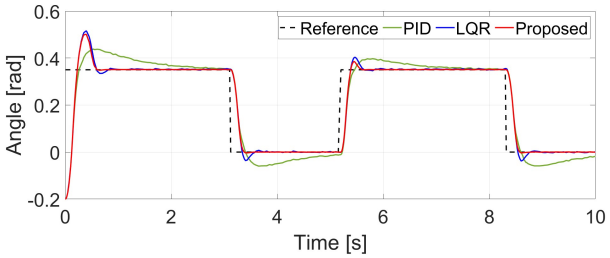

Fig. 6. Third scenario: trajectory tracking

- Trajectory tracking of a sinusoidal signal. The desired trajectory is defined by

$$\phi_d(t) = 0.5 \sin t + 0.2 \cos 3t. \tag{29}$$

Fig. 7 shows the three control algorithms. The PID control shows an oscillatory response, contains fluctuations, and is not robust to external disturbances. The LQR control presents a similar response to the proposed controller. However, the calculation cost is high. The proposed control performs superior to the PID and LQR control; see table II. In addition to presenting advantages in practical implementation by not saturating the operating range in the actuators.

B. Experimental Results

First, the angle $\phi(t)$ is estimated using the $MPU - 6050$ inertial measurement unit and the Kalman filter. The control is calculated by generating a virtual control input Ω_d, which is a reference for the PID control. Finally, the PID control is calculated by reading the encoders of each DC motor; this PID

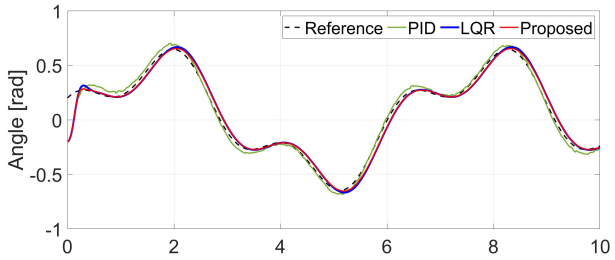

Fig. 7. Third scenario: trajectory tracking

TABLE II
THE SIMULATION PERFORMANCE INDEX FOR QUADRATIC TRAJECTORY.

Controller	ISE	ITSE	IAE	ITAE
The simulation performance index for quadratic trajectory				
PID	0.0801	0.2516	0.4831	1.9891
LQR	0.0722	0.2005	0.2696	0.8905
$Proposed$	0.0603	0.1959	0.2436	0.7839
The simulation performance index for sin trajectory				
PID	0.03328	0.08481	0.4091	1.7563
LQR	0.03262	0.08358	0.3973	1.6871
$Proposed$	0.0297	0.6921	0.3343	1.5160

control generates the PWM signals of the DC motors, Fig. 3 shows the proposed control scheme. Real-time tests are carried out to validate the control architecture based on ROS design. The control is implemented in the ESP32 microcontroller.

The ROS nodes, the complementary filter, and the control have been programmed in C++. Two scenarios have been addressed, the stabilization of the equilibrium point and the ability to reject external disturbances and keep the pendulum stabilized in a vertical position. Figs. 8 and 9 show the angular position and angular velocity. The Figs show that the control algorithm effectively maintains the equilibrium positions within about 0.1 radians (5 degrees). Despite the elements of friction, noise, and external disturbances, the control shows a smooth and robust response.

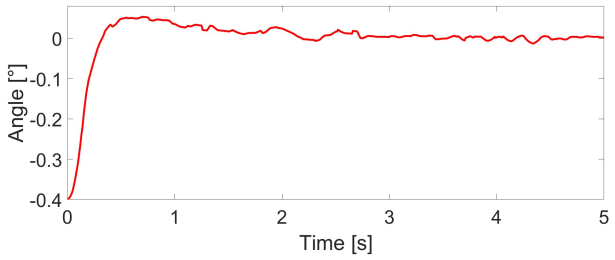

Fig. 8. Experimental results performance response of the controller. ϕ(t)

In a second scenario, the ability to reject disturbances is tested. Figs. 10 and 11 show how the system has been disturbed externally in 6 and 12 seconds. Despite being an LTI control, it manages to stabilize the bar to the vertical axis despite this disturbance. The robot's operation can be

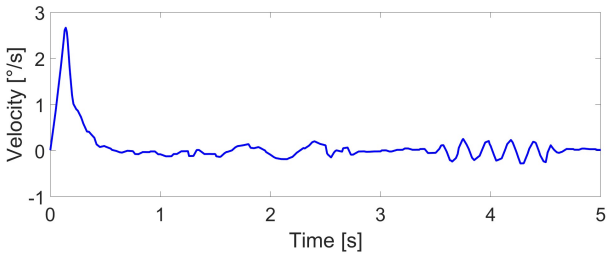

Fig. 9. Experimental results performance response of the controller. $\dot{\phi}$(t)

shown in the following link https://youtu.be/L1eUwG2GSfo. The control algorithm is lightweight, and robust, and can stabilize the self-balancing two-wheeled robot. Proposing ROS middleware to the embedded system allows adding modules such as navigation, manipulation, and perception. Which will allow surveillance, delivery, transfer of objects, and autonomous navigation tasks indoors or outdoors.

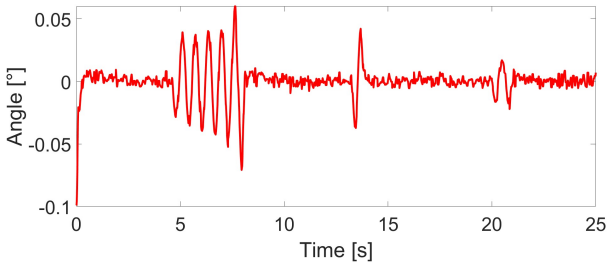

Fig. 10. Experimental results performance response of the controller subject to external disturbances. ϕ(t)

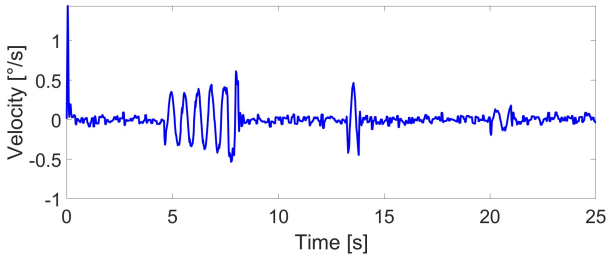

Fig. 11. Experimental results performance response of the controller subject to external disturbances. $\dot{\phi}$(t)

VI. Conclusion and Future Work

This article designs a ROS-based architecture to control a two-wheeled self-balancing robot. The ROS architecture is open and allows the integration of different modules, such as mapping, navigation, perception, and manipulation, to develop new applications. This architecture can be a starting point for designing new robotics apps. The bounded saturation control shows robustness against small bounded external disturbances, as well as better performance in path-following control compared to classical PID and LQR controls. Besides that, its implementation is simple and light computing. However, we are the noise in the Kalman filter; friction and wear of the actuators can generate a small region of attraction and oscillation. In future work, control will be designed using ADRC's disturbance rejection control methodology, which estimates endogenous and exogenous disturbances through an extended state observer and attenuates them under feedback.

References

[1] A. Stefek, T. V. Pham, V. Krivanek and K. L. Pham, "Energy Comparison of Controllers Used for a Differential Drive Wheeled Mobile Robot," in IEEE Access, vol. 8, pp. 170915-170927, 2020, doi: 10.1109/ACCESS.2020.3023345.

[2] Y. Maddahi and K. Zareinia, "Nonparametric Bootstrap Technique to Improve Positional Accuracy in Mobile Robots With Differential Drive Mechanism," in IEEE Access, vol. 8, pp. 158502-158511, 2020, doi: 10.1109/ACCESS.2020.3020864.

[3] U. Ruiz, "Capturing a Dubins Car With a Differential Drive Robot," in IEEE Access, vol. 10, pp. 81805-81815, 2022, doi: 10.1109/ACCESS.2022.3196342.

[4] Q. Lu, Z. Li, H. Song and C. -Y. Su, "Visual Regulation of Differential-Drive Mobile Robots: A Nonadaptive Switching Approach," in IEEE Transactions on Systems, Man, and Cybernetics: Systems, vol. 51, no. 11, pp. 6874-6884, Nov. 2021, doi: 10.1109/TSMC.2020.2963889.

[5] F. Ke, Z. Li and C. Yang, "Robust Tube-Based Predictive Control for Visual Servoing of Constrained Differential-Drive Mobile Robots," in IEEE Transactions on Industrial Electronics, vol. 65, no. 4, pp. 3437-3446, April 2018, doi: 10.1109/TIE.2017.2756595.

[6] R. Mao and H. Dai, "Distributed Non-Convex Model Predictive Control for Non-Cooperative Collision Avoidance of Networked Differential Drive Mobile Robots," in IEEE Access, vol. 10, pp. 52674-52685, 2022, doi: 10.1109/ACCESS.2021.3134696.

[7] R. F. Carpio et al., "A Navigation Architecture for Ackermann Vehicles in Precision Farming," in IEEE Robotics and Automation Letters, vol. 5, no. 2, pp. 1103-1110, April 2020, doi: 10.1109/LRA.2020.2967306.

[8] Y. Gao, Y. Shen, T. Xu, W. Zhang and L. Güvenç, "Oscillatory Yaw Motion Control for Hydraulic Power Steering Articulated Vehicles Considering the Influence of Varying Bulk Modulus," in IEEE Transactions on Control Systems Technology, vol. 27, no. 3, pp. 1284-1292, May 2019, doi: 10.1109/TCST.2018.2803746.

[9] L. Bascetta, D. A. Cucci, and M. Matteucci "Kinematic trajectory tracking controller for an all-terrain Ackermann steering vehicle," IFAC-PapersOnLine, vol. 49, no. 15, pp. 13-18, 2016.

[10] S. Upadhyay and A. Ratnoo, "A Point-to-Ray Framework for Generating Smooth Parallel Parking Maneuvers," in IEEE Robotics and Automation Letters, vol. 3, no. 2, pp. 1268-1275, April 2018, doi: 10.1109/LRA.2018.2795655.

[11] M. T. Watson, D. T. Gladwin and T. J. Prescott, "Collinear Mecanum Drive: Modeling, Analysis, Partial Feedback Linearization, and Nonlinear Control," in IEEE Transactions on Robotics, vol. 37, no. 2, pp. 642-658, April 2021, doi: 10.1109/TRO.2020.2977878.

[12] D. U. Rijalusalam and I. Iswanto, "Implementation Kinematics Modeling and Odometry of Four Omni Wheel Mobile Robot on The Trajectory Planning and Motion Control Based Microcontroller," Journal of Robotics and Control (JRC), vol. 2, no. 5, pp. 448-455, 2021.

[13] R. T. Yunardi, D. Arifianto, F. Bachtiar, and J. I. Prananingrum, "Holonomic Implementation of Three Wheels Omnidirectional Mobile Robot using DC Motors," Journal of Robotics and Control (JRC), vol. 2, no. 2, 2021, doi: 10.18196/jrc.2254.

[14] A. Neaz, S. Lee, and K. Nam, "Design and Implementation of an Integrated Control System for Omnidirectional Mobile Robots in Industrial Logistics," Sensors, vol. 23, no. 6, p. 3184, 2023, doi: 10.3390/s23063184

[15] T. Terakawa, M. Komori, K. Matsuda and S. Mikami, "A Novel Omnidirectional Mobile Robot With Wheels Connected by Passive Sliding Joints," in IEEE/ASME Transactions on Mechatronics, vol. 23, no. 4, pp. 1716-1727, Aug. 2018, doi: 10.1109/TMECH.2018.2842259.

[16] S. Lee and D. Chwa, "Dynamic Image-Based Visual Servoing of Monocular Camera Mounted Omnidirectional Mobile Robots Considering Actuators and Target Motion via Fuzzy Integral Sliding Mode Control," in IEEE Transactions on Fuzzy Systems, vol. 29, no. 7, pp. 2068-2076, July 2021, doi: 10.1109/TFUZZ.2020.2985931.

[17] K. Albert, K. S. Phogat, F. Anhalt, R. N. Banavar, D. Chatterjee and B. Lohmann, "Structure-Preserving Constrained Optimal Trajectory Planning of a Wheeled Inverted Pendulum," in IEEE Transactions on Robotics, vol. 36, no. 3, pp. 910-923, June 2020, doi: 10.1109/TRO.2020.2985579.

[18] W. Zhao, X. Wang, B. Qi and T. Runge, "Ground-Level Mapping and Navigating for Agriculture Based on IoT and Computer Vision," in IEEE Access, vol. 8, pp. 221975-221985, 2020, doi: 10.1109/ACCESS.2020.3043662.

[19] X. Gao et al., "Review of Wheeled Mobile Robots' Navigation Problems and Application Prospects in Agriculture," in IEEE Access, vol. 6, pp. 49248-49268, 2018, doi: 10.1109/ACCESS.2018.2868848.

[20] J. Pak, J. Kim, Y. Park and H. I. Son, "Field Evaluation of Path-Planning Algorithms for Autonomous Mobile Robot in Smart Farms," in IEEE Access, vol. 10, pp. 60253-60266, 2022, doi: 10.1109/ACCESS.2022.3181131.

[21] W. Wan, B. Shi, Z. Wang and R. Fukui, "Multirobot Object Transport via Robust Caging," in IEEE Transactions on Systems, Man, and Cybernetics: Systems, vol. 50, no. 1, pp. 270-280, Jan. 2020, doi: 10.1109/TSMC.2017.2733552.

[22] J. Alonso-Mora, S. Baker, and D. Rus, "Multi-robot formation control and object transport in dynamic environments via constrained optimization," The International Journal of Robotics Research, vol. 36, no. 9, pp. 1000-1021, 2017, doi:10.1177/0278364917719333

[23] H. M. Pérez-Villeda, G. Arechavaleta, A. Morales-Díaz, "Multi-vehicle coordination based on hierarchical quadratic programming," Control Engineering Practice, vol. 94, p. 104206, 2020.

[24] D. Koung, O. Kermorgant, I. Fantoni and L. Belouaer, "Cooperative Multi-Robot Object Transportation System Based on Hierarchical Quadratic Programming," in IEEE Robotics and Automation Letters, vol. 6, no. 4, pp. 6466-6472, Oct. 2021, doi: 10.1109/LRA.2021.3092305.

[25] C. L. Shih and L. C. Lin, "Trajectory Planning and Tracking Control of a Differential-Drive Mobile Robot in a Picture Drawing Application," Robotics, vol. 6, no. 3, p. 17, 2017, doi: 10.3390/robotics6030017.

[26] X. Hou et al., "A Novel Mobile Robot Navigation Method Based on Hand-Drawn Paths," in IEEE Sensors Journal, vol. 20, no. 19, pp. 11660-11673, 1 Oct.1, 2020, doi: 10.1109/JSEN.2020.2997055.

[27] Kaneko, R., Nakamura, Y., Morita, R. et al. Point cloud data map creation from factory design drawing for LiDAR localization of an autonomous mobile robot. Artif Life Robotics (2022). https://doi.org/10.1007/s10015-022-00834-y

[28] D. Lee, G. Kang, B. Kim and D. H. Shim, "Assistive Delivery Robot Application for Real-World Postal Services," in IEEE Access, vol. 9, pp. 141981-141998, 2021, doi: 10.1109/ACCESS.2021.3120618.

[29] V. P. Bacheti, A. S. Brandão and M. Sarcinelli-Filho, "A Path-Following Controller for a UAV-UGV Formation Performing the Final Step of Last-Mile-Delivery," in IEEE Access, vol. 9, pp. 142218-142231, 2021, doi: 10.1109/ACCESS.2021.3120347.

[30] J. G. Parada-Salado, L. E. Ortega-Garcia, L. F. Ayala-Ramirez, F. J. Perez-Pinal, C. A. Herrera-Ramirez and J. A. Padilla-Medina, "A Low-Cost Land Wheeled Autonomous Mini-robot for In-door Surveillance," in IEEE Latin America Transactions, vol. 16, no. 5, pp. 1298-1305, May 2018, doi: 10.1109/TLA.2018.8407100.

[31] T. Wang, P. Huang and G. Dong, "Cooperative Persistent Surveillance on a Road Network by Multi-UGVs With Detection Ability," in IEEE Transactions on Industrial Electronics, vol. 69, no. 11, pp. 11468-11478, Nov. 2022, doi: 10.1109/TIE.2021.3121729.

[32] C. Li, C. Fang, F. Wang, B Xia, and Y Song "Complete coverage path planning for an Arnold system based mobile robot to perform specific types of missions," Front Inform Technol Electron Eng, vol. 20, pp. 1530–1542, 2019, doi: 10.1631/FITEE.1800616.

[33] A. H. Tan and G. Nejat, "Enhancing Robot Task Completion Through Environment and Task Inference: A Survey from the Mobile Robot Perspective," J Intell Robot Syst, vol. 106, no. 73, 2022, doi: 10.1007/s10846-022-01776-0

[34] F. Niroui, K. Zhang, Z. Kashino and G. Nejat, "Deep Reinforcement Learning Robot for Search and Rescue Applications: Exploration in Unknown Cluttered Environments," in IEEE Robotics and Automation Letters, vol. 4, no. 2, pp. 610-617, April 2019, doi: 10.1109/LRA.2019.2891991.

[35] C. Wang, J. Cheng, J. Wang, X. Li and M. Q. H. Meng, "Efficient Object Search With Belief Road Map Using Mobile Robot," in IEEE Robotics and Automation Letters, vol. 3, no. 4, pp. 3081-3088, Oct. 2018, doi: 10.1109/LRA.2018.2849610.

[36] G. Curiel-Olivares, J. Linares-Flores, A. Hernández-Méndez, J. F. Guerrero-Castellanos, G. Mino-Aguilar and C. García-Rodríguez, "Two-In-Wheeled Self-Balancing Electric Vehicle Based on Active Disturbance Rejection Controller," 2019 IEEE International Conference on Mechatronics (ICM), Ilmenau, Germany, 2019, pp. 608-613, doi: 10.1109/ICMECH.2019.8722948.

[37] G. Curiel-Olivares, J. Linares Flores, J. F. Guerrero-Castellanos, and A. Hernández-Méndez, "Self-balancing based on Active Disturbance Rejection Controller for the Two-In-Wheeled Electric Vehicle, Experimental results," Mechatronics, vol. 76, p. 102552, 2021, doi: 10.1016/j.mechatronics.2021.102552.

[38] Y. Zhang, K. Song, J. Yi, P. Huang, Z. Duan and Q. Zhao, "Absolute Attitude Estimation of Rigid Body on Moving Platform Using Only Two Gyroscopes and Relative Measurements," in IEEE/ASME Transactions on Mechatronics, vol. 23, no. 3, pp. 1350-1361, June 2018, doi: 10.1109/TMECH.2018.2811730.

[39] K. M. Goher and S. O. Fadlallah, "Control of a Two-wheeled Machine with Two-directions Handling Mechanism Using PID and PD-FLC Algorithms," Int. J. Autom. Comput., vol. 16, pp. 511–533, 2019, doi: 10.1007/s11633-019-1172-0.

[40] H. Ren and C. Zhou, "Control System of Two-Wheel Self-Balancing Vehicle," J. Shanghai Jiaotong Univ. (Sci.), vol. 26, pp. 713–721, 2021, doi: 10.1007/s12204-021-2361-x.

[41] C. Iwendi, M. A. Alqarni, J. H. Anajemba, A. S. Alfakeeh, Z. Zhang and A. K. Bashir, "Robust Navigational Control of a Two-Wheeled Self-Balancing Robot in a Sensed Environment," in IEEE Access, vol. 7, pp. 82337-82348, 2019, doi: 10.1109/ACCESS.2019.2923916.

[42] J. Diaz-Tellez, V. Gutierrez-Vicente, J. Estevez-Carreon, O. D. Ramirez-Cardenas, and R. S. Garcia-Ramirez, "Nonlinear Control of a Two-Wheeled Self-balancing Autonomous Mobile Robot," Advances in Soft Computing: 20th Mexican International Conference on Artificial Intelligence, pp. 348-359, 2021, doi: 10.1007/978-3-030-89820-5_28.

[43] A. Lima-Pérez et al., "Robust Control of a Two-Wheeled Self-Balancing Mobile Robot," 2021 International Conference on Mechatronics, Electronics and Automotive Engineering (ICMEAE), Cuernavaca, Mexico, 2021, pp. 196-201, doi: 10.1109/ICMEAE55138.2021.00038.

[44] R. Xiong, L. Li, C. Zhang, K. Ma, X. Yi and H. Zeng, "Path Tracking of a Four-Wheel Independently Driven Skid Steer Robotic Vehicle Through a Cascaded NTSM-PID Control Method," in IEEE Transactions on Instrumentation and Measurement, vol. 71, pp. 1-11, 2022, Art no. 7502311, doi: 10.1109/TIM.2022.3160549.

[45] S. Kim and S. Kwon, "Nonlinear Optimal Control Design for Underactuated Two-Wheeled Inverted Pendulum Mobile Platform," in IEEE/ASME Transactions on Mechatronics, vol. 22, no. 6, pp. 2803-2808, Dec. 2017, doi: 10.1109/TMECH.2017.2767085.

[46] F. A Jiménez, I. Ruge, and A. A Jiménez, "Modeling and Control of a Two Wheeled Self-Balancing Robot: a didactic platform for control engineering education," Proceedings of the 18th LACCEI International Multi-Conference for Engineering, Education and Technology, 2020, doi: 10.18687/LACCEI2020.1.1.556.

[47] S. M. H. Rostami, A. K. Sangaiah, J. Wang, and H. Kim, "Real-time obstacle avoidance of mobile robots using state-dependent Riccati equation approach," J Image Video Proc., 2018, doi: 10.1186/s13640-018-0319-1.

[48] H. Tourajizadeh, M. Rezaei, and A. H. Sedigh, "Optimal Control of Screw In-pipe Inspection Robot with Controllable Pitch Rate," J Intell

Robot Syst, vol. 90, pp. 269–286, 2018, doi: 10.1007/s10846-017-0658-7.

[49] T. Johnson, S. Zhou, W. Cheah, W. Mansell, R. Young, and S Watson "Implementation of a Perceptual Controller for an Inverted Pendulum Robot," J Intell Robot Syst, vol. 99, pp. 683–692, 2020, doi: 10.1007/s10846-020-01158-4.

[50] S. Jeong and T. Takahashi, "Wheeled inverted pendulum type assistant robot: design concept and mobile control," Intel Serv Robotics, vol. 1, no. 4, pp. 313–320, 2008, doi: 10.1007/s11370-008-0024-5

[51] X. Zhang, R. Wang, Y. Fang, B. Li and B. Ma, "Acceleration-Level Pseudo-Dynamic Visual Servoing of Mobile Robots With Backstepping and Dynamic Surface Control," in IEEE Transactions on Systems, Man, and Cybernetics: Systems, vol. 49, no. 10, pp. 2071-2081, Oct. 2019, doi: 10.1109/TSMC.2017.2777897.

[52] Y. Chen, N. Li, W. Zeng, S. Zhang and G. Ma, "Curved Path Following Controller for 4W Skid-Steering Mobile Robots Using Backstepping," in IEEE Access, vol. 10, pp. 66072-66082, 2022, doi: 10.1109/ACCESS.2022.3185062.

[53] R. Parween, M. V. Heredia, M. M. Rayguru, R. E. Abdulkader and M. R. Elara, "Autonomous Self-Reconfigurable Floor Cleaning Robot," in IEEE Access, vol. 8, pp. 114433-114442, 2020, doi: 10.1109/ACCESS.2020.2999202.

[54] C. -H. Chiu and C. -Y. Wu, "Bicycle Robot Balance Control Based on a Robust Intelligent Controller," in IEEE Access, vol. 8, pp. 84837-84849, 2020, doi: 10.1109/ACCESS.2020.2992792.

[55] X. Yang, P. Wei, Y. Zhang, X. Liu and L. Yang, "Disturbance Observer Based on Biologically Inspired Integral Sliding Mode Control for Trajectory Tracking of Mobile Robots," in IEEE Access, vol. 7, pp. 48382-48391, 2019, doi: 10.1109/ACCESS.2019.2907126.

[56] I. Reguii, I. Hassani, and C. Rekik, "Mobile Robot Navigation Using Planning Algorithm and Sliding Mode Control in a Cluttered Environment," Journal of Robotics and Control (JRC), vol. 3, no. 2, pp. 166-175, 2022.

[57] N. Esmaeili, A. Alfi, and H. Khosravi, "Balancing and Trajectory Tracking of Two-Wheeled Mobile Robot Using Backstepping Sliding Mode Control: Design and Experiments," J Intell Robot Syst, vol. 87, pp. 601–613, 2017, doi: 10.1007/s10846-017-0486-9.

[58] H. Xie, J. Zheng, Z. Sun, H. Wang, and R. Chai "Finite-time tracking control for nonholonomic wheeled mobile robot using adaptive fast nonsingular terminal sliding mode," Nonlinear Dyn, vol. 110, pp. 1437–1453, 2022 doi: 10.1007/s11071-022-07682-2.

[59] M. Cui, "Observer-Based Adaptive Tracking Control of Wheeled Mobile Robots With Unknown Slipping Parameters," in IEEE Access, vol. 7, pp. 169646-169655, 2019, doi: 10.1109/ACCESS.2019.2955887

[60] J. Meng, H. Xiao, L. Jiang, Z. Hu, L. Jiang, and N. Jiang, "Adaptive Model Predictive Control for Mobile Robots with Localization Fluctuation Estimation" Sensors, vol. 23, no. 5, p. 2501, 2023, doi: 10.3390/s23052501.

[61] J. Lin, Z. Miao, H. Zhong, W. Peng, Y. Wang and R. Fierro, "Adaptive Image-Based Leader–Follower Formation Control of Mobile Robots With Visibility Constraints," in IEEE Transactions on Industrial Electronics, vol. 68, no. 7, pp. 6010-6019, July 2021, doi: 10.1109/TIE.2020.2994861.

[62] D. Chwa and J. Boo, "Adaptive Fuzzy Output Feedback Simultaneous Posture Stabilization and Tracking Control of Wheeled Mobile Robots With Kinematic and Dynamic Disturbances," in IEEE Access, vol. 8, pp. 228863-228878, 2020, doi: 10.1109/ACCESS.2020.3046282

[63] M. Cui, "Observer-Based Adaptive Tracking Control of Wheeled Mobile Robots With Unknown Slipping Parameters," in IEEE Access, vol. 7, pp. 169646-169655, 2019, doi: 10.1109/ACCESS.2019.2955887.

[64] M. Cui, W. Liu, H. Liu, H. Jiang, and Z. Wang, "Extended state observer-based adaptive sliding mode control of differential-driving mobile robot with uncertainties," Nonlinear Dyn, vol. 83, pp. 667–683, 2016, doi: 10.1007/s11071-015-2355-z.

[65] K. Liu, H. Gao, H. Ji, and Z. Hao, "Adaptive Sliding Mode Based Disturbance Attenuation Tracking Control for Wheeled Mobile Robots," Int. J. Control Autom. Syst., vol. 18, pp. 1288–1298, 2020, doi: 10.1007/s12555-019-0262-7

[66] C. F. Hsu and W. F. Kao, "Double-loop fuzzy motion control with CoG supervisor for two-wheeled self-balancing assistant robots," Int. J. Dynam. Control, vol. 8, pp. 851–866, 2020, doi: 10.1007/s40435-020-00617-y.

[67] M. Moness, D. Mahmoud, and A. Hussein, "Real-time Mamdani-like fuzzy and fusion-based fuzzy controllers for balancing two-wheeled inverted pendulum," J Ambient Intell Human Comput, vol. 13, pp. 3577–3593, 2022, doi: 10.1007/s12652-020-01991-3

[68] T. Zhao, Q. Yu, S. Dian, R. Guo and S. Li, "Non-singleton General Type-2 Fuzzy Control for a Two-Wheeled Self-Balancing Robot," Int. J. Fuzzy Syst., vol. 21, pp. 1724–1737, 2019, doi: 10.1007/s40815-019-00664-4.

[69] T. A. Mai, D. N. Anisimov, T. S. Dang, V. N. Dinh, "Development of a microcontroller-based adaptive fuzzy controller for a two-wheeled self-balancing robot," Microsystem Technologies, vol. 24, 2018, doi: 10.1007/s00542-018-3825-2.

[70] L. Gentilini, S. Rossi, D. Mengoli, A. Eusebi and L. Marconi, "Trajectory Planning ROS Service for an Autonomous Agricultural Robot," 2021 IEEE International Workshop on Metrology for Agriculture and Forestry (MetroAgriFor), Trento-Bolzano, Italy, 2021, pp. 384-389, doi: 10.1109/MetroAgriFor52389.2021.9628620.

[71] J. Martin et al., "A Generic ROS-Based Control Architecture for Pest Inspection and Treatment in Greenhouses Using a Mobile Manipulator," in IEEE Access, vol. 9, pp. 94981-94995, 2021, doi: 10.1109/ACCESS.2021.3093978.

[72] M. S. Miah and J. Knoll, "Area Coverage Optimization Using Heterogeneous Robots: Algorithm and Implementation," in IEEE Transactions on Instrumentation and Measurement, vol. 67, no. 6, pp. 1380-1388, June 2018, doi: 10.1109/TIM.2018.2800178.

[73] W. Guan, S. Chen, S. Wen, Z. Tan, H. Song and W. Hou, "High-Accuracy Robot Indoor Localization Scheme Based on Robot Operating System Using Visible Light Positioning," in IEEE Photonics Journal, vol. 12, no. 2, pp. 1-16, April 2020, Art no. 7901716, doi: 10.1109/JPHOT.2020.2981485.

[74] R. Valner, V. Vunder, A. Aabloo, M. Pryor and K. Kruusamäe, "TeMoto: A Software Framework for Adaptive and Dependable Robotic Autonomy With Dynamic Resource Management," in IEEE Access, vol. 10, pp. 51889-51907, 2022, doi: 10.1109/ACCESS.2022.3173647.

[75] R. F. Carpio et al., "A Navigation Architecture for Ackermann Vehicles in Precision Farming," in IEEE Robotics and Automation Letters, vol. 5, no. 2, pp. 1103-1110, April 2020, doi: 10.1109/LRA.2020.2967306.

[76] M. Pei, H. An, B. Liu and C. Wang, "An Improved Dyna-Q Algorithm for Mobile Robot Path Planning in Unknown Dynamic Environment," in IEEE Transactions on Systems, Man, and Cybernetics: Systems, vol. 52, no. 7, pp. 4415-4425, July 2022, doi: 10.1109/TSMC.2021.3096935.

[77] F. Ugalde Pereira, P. Medeiros de Assis Brasil, M. A. de Souza Leite Cuadros, A. R. Cukla, P. Drews Junior and D. F. Tello Gamarra, "Analysis of Local Trajectory Planners for Mobile Robot with Robot Operating System," in IEEE Latin America Transactions, vol. 20, no. 1, pp. 92-99, Jan. 2022, doi: 10.1109/TLA.2022.9662177.

[78] J. Mišeikis et al., "Lio-A Personal Robot Assistant for Human-Robot Interaction and Care Applications," in IEEE Robotics and Automation Letters, vol. 5, no. 4, pp. 5339-5346, Oct. 2020, doi: 10.1109/LRA.2020.3007462.

[79] J. Li, M. Liu, W. Wang and C. Hu, "Inspection Robot Based on Offline Digital Twin Synchronization Architecture," in IEEE Journal of Radio Frequency Identification, vol. 6, pp. 943-947, 2022, doi: 10.1109/JRFID.2022.3207047.

[80] M. A. Chung and C. W. Lin, "An Improved Localization of Mobile Robotic System Based on AMCL Algorithm," in IEEE Sensors Journal, vol. 22, no. 1, pp. 900-908, no. 1, 2022, doi: 10.1109/JSEN.2021.3126605.

[81] A. Bihlmaier and H. Wörn, Hands-on Learning of ROS using Common Hardware, 2015.